Batch Equilibrium, Kinetics and Thermodynamics Study of Sulfamethoxazole antibiotics onto *Azolla filiculoides* as a Novel Biosorbent

Abstract: *Azolla filiculoides* (AF) were used as adsorbent for the sorption of Sulfamethoxazole (SMZ) from aqueous solution. Also adsorption Isotherms, kinetics and thermodynamics were studied. Experiments were conducted by varying parameters such as contact time, agitation speed, initial SMZ concentration and temperature. Adsorption isotherms models including Langmuir, Freundlich and Temkin were tested. It was inferred that the Langmuir models (with very high R^2 values) were most suited to describe the sorption of SMZ in aqueous solutions. The experimental data were fitted into the following kinetic models: pseudo-first-order, pseudo-second-order, and the intraparticle diffusion model. It was observed that the pseudo-second-order kinetic model described the adsorption process better than other kinetic models. Thermodynamic parameters including the Standard free energy changes (ΔG°), standard enthalpy change (ΔH°), and standard entropy change (ΔS°) were calculated. This parameters indicated that the adsorption of SMZ onto AF biomass was feasible, spontaneous and endothermic. This study revealed that AF biomass is a good adsorbent for the elimination of Sulfamethoxazole antibiotics from aqueous solution.
Keywords: Sulfamethoxazole, *Azolla filiculoides*, Adsorption Isotherm, Kinetics, Thermodynamics

Introduction: Since the use of the drugs has significantly increased for the human and animals in recent decades and they can simply release into environment, these chemical and their metabolites has found more attention as an important risk for environment (1, 2). sulfamethoxazole (SMZ) is an important bacteriostatic agent that is commonly used in human and veterinary medicine (3, 4). The release of SMZ into the ecosystem or wastewater effluents has caused pollution and many human diseases (5, 6).

The conventional wastewater treatment plants (WWTPs) were not designed to remove the antibiotic and they are not effective for this purpose (7, 8); thus, these chemicals are incompletely removed and released into aquatic environment (9). This has generated great concern because it may lead to the development of antibiotic-resistant bacteria and potential endocrine disrupting compounds (10, 11).

Various treatment technologies have been proposed for antibiotics removal including chemical oxidation, precipitation, biological treatment, ion exchange, coagulation–flocculation and so on (12, 13). However, these treatment processes present a number of drawbacks in terms of low efficiency and producing large amounts of sludge which can diminish the effective use of these methods to treat (14-16).

Among these methods, the adsorption method has the advantages of easy operation, low cost, high efficiency; it is considered as one of the most promising technologies (17, 18). The efficiency of the adsorption processes is extremely affected by the type of adsorbent and adsorbate properties such as surface area, porosity, and pore diameter (19, 20). Several materials have been used as adsorbents for the removal of antibiotics from aqueous solution including carbon adsorbents(21-24), clay and mineral(25), polymeric resins(26), and other adsorbents such as metals and their oxides(27, 28), molecular imprinted polymers(29), mesoporous material(30), chitosan(31), gels(32) and agricultural wastes such as Lemna minor and Canola and etc(18, 33).

Azolla filiculoides is a floating water fern and quickly growth which it can be observed over the water surface and formed a dense mat; therefore it can cause numerous unenthusiastic effects for marine life (34, 35). However, the use of *Azolla filiculoides* as a biosorbent to remove pollutant from industrial effluents would be a "win–win" for both environmental problems, because it would be effective in pollutant removal, as well as elimination the problem associated with the rapid growth of this plant (36, 37). Recently, non-living *Azolla filiculoides* has been used as a potential biosorbent to remove the heavy metal (38), phenol compounds (39, 40 and dyes (41, 42). The scientists have also reported that *Azolla filiculoides* is capable for removing these compounds from aqueous solution. In this study, the dried *Azolla filiculoides* (AF) was used as a biosorbent to remove SMZ as a target pollutant from aqueous solution. The aim of study was to evaluate the biosorption of SMZ on AF using batch experiments under different experimental conditions, including agitation speed, pH, contact time, temperature and initial SMZ concentrations. In addition, isotherm, kinetic and thermodynamic of the SMZ adsorption on to AF were studied.

Materials and methods

The Sulfamethoxazole (99%) (CAS Number=723-46-6; chemical formula: $C_{10}H_{11}N_3O_3S$; molecular weight=253.279 g/mol; maximum wavelength =267 nm**)** were obtained from Sigma-Aldrich Ltd., USA and used without any further purification. The chemical structure is shown in Fig. 1. All the other chemicals were obtained from Merck Co. (Germany). All the chemicals used for the study were of analytical grade.

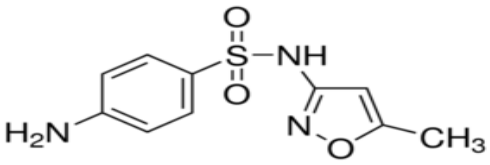

Fig. 1. The chemical structure of Sulfamethoxazole

Preparation of Adsorbent:

Azolla filiculoides were collected from Anzali wetland, Iran. The collected AF was washed with distilled water. Then they were cut into small pieces and dried in hot air oven at 100˚C for 24 h to remove moisture. The dried samples were ground and powdered. The biomass was treated with 0.5 M H_2SO_4 for 2 h followed by washing with distilled water and then dried in 100˚C for 24 h. The separated samples were weighed and sealed with zip-lock bags for the further analysis of adsorption studies.

The morphological features and surface characteristics AF before and after use were examined using an environmental scanning electron microscopy (ESEM) instrument (Philips XL30). The specific surface area of adsorbent was determined by the BET method using the Gemini 2357 of micrometrics Co. The compositions of AF biomass were examined using XRD (X' Pert Pro, PANalytical, Netherlands) with Cu Kα radiation at 40 kV and 40 mA. The scanned range was 2θ of 10–60° with a step size of 2θ of 0.05°.

Batch experimental procedure: Various experimental conditions which may influence the biosorption of SMZ on AF including Contact time, pH, biosorbent dosage and initial SMZ concentration were tested using batch experiments. Initial SMZ solutions with different concentrations were prepared by diluting a SMZ stock standard solution of 1000 mg/L with

distilled water. All glassware and plastics were soaked in 10% (v/v) nitric acid solution for 1 day before use and then cleaned repeatedly with deionized water. The solution pH was adjusted using either diluted 0.1 M HCL or 0.1 M NaOH solution. In the adsorption experiment, content of the biosorbent was added to a standard-joint pyrex glass bottle (250 ml) containing 100 ml wastewater sample with concentration 10-100 mg/L and at the desired pH=7. The tube was then shaken at 250 rpm on an electrically thermostatic reciprocating shaker for 90 min. The equilibrium times at four different temperatures (293, 303, 313, and 323 K) were estimated by testing the samples collected at different time intervals until the SMZ content in the sample was constant. After equilibrium, the suspension was filtered through 0.45 μm nitrocellulose membrane. SMZ analysis was performed using an Agilent 1200 series HPLC equipped with a C18 column, a UV detector (at wavelength 267 nm), and a methanol/water (50/50 v/v) mobile phase at a flow rate of 0.6 ml/min. The content of SMZ biosorbed on dried AF was estimated by the difference between the initial and final SMZ concentrations remained in the supernatant. All experiments were conducted in triplicate and the averages of the results are presented in this study. The equilibrium removal capacity was calculated by (43):

$$q_e = (C_0 - C_e)\frac{V}{M}$$

Where q_e (mg/g) is the equilibrium adsorption capacity, C_e is the antibiotic concentration at equilibrium (mg/L), V is the volume of solution (L) and w is the mass of adsorbent (g).

Results and Discussion:

It was found that the specific surface area of AF is 36 m^2/g. The morphology of single AF was investigated using SEM and the image is shown in Fig. 1a. This Fig shows the surface texture and porosity of the AF particle. Also, it reveals that the particles have a very narrow size distribution, spherical shaped with very small holes and rough surfaces. In contrast, Fig. 1(b) discloses that the clear pore textural structure is not observed on the surface of AF after adsorption process which could be due to either agglomeration on the surface or the incursion of SMZ into the pores of AF.

X-ray diffraction (XRD) patterns of AF biomass before (a) and after (b) use, show the same diffused peak with maximum at 2θ 21.1◦ and 21.4◦, respectively (Fig. 2). However, AF after use shows a higher intensity attributed to SMZ biosorbtion on the surface of AF biomass.

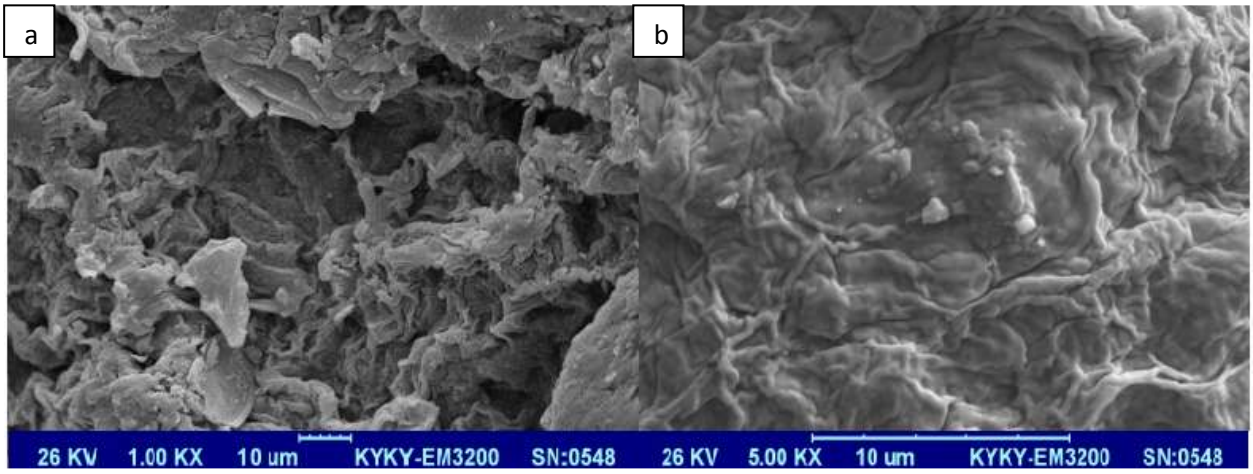

Fig.1: SEM image of AF biomass a: before used b: after used

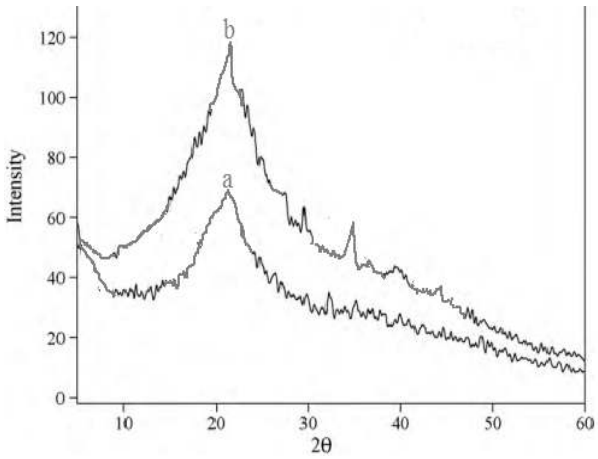

Fig. 2: XRD patterns of AF biomass a: before used b: after used

Effect of pH: The effect of pH for the adsorption of SMZ onto AF is shown in Fig. 3. It can be seen that the adsorption of SMZ was pH-dependent. The results show that the amount of adsorbed SMZ onto AF decreases as the pH increases from 6 to 11. This situation can be related to the surface charge of the adsorbent. AF has negatively charged adsorption sites, but it is positively charged at low pH values(40). Therefore the electrostatic interactions between negatively charged groups in the SMZ molecule and the positively charged adsorbent increase. Also SMX predominantly occurs in its neutral form, appearing in relatively acidic solutions where its pKa value (5.64) corresponds to the average pH level of surface water(3, 7). Since the pH in surface water falls between 6 and 10, the negatively-charged form of SMX also appears often. The aniline group on the molecule has a negative charge on the nitrogen atom, which acts as an ionic binding site. Also AF has negatively charged adsorption sites at high pH, Therefore the electrostatic interactions between negatively charged groups in the SMZ molecule and the negatiely charged adsorbent decreaced. Also this behaviour can be explained by the zero point charge of the adsorbent and obtained in previous studies (pH_{ZPC}= 6.5)(36, 40). At a pH above this zero point charge, the surface of the adsorbent becomes negatively charged, and declines the adsorption of negatively charged SMZ through the decreace electrostatic force of attraction.

Effect of agitation speed

The study of the effect of agitation speed on the adsorption of SMZ from aqueous solution was conducted by varying agitation speed from 50 to 400 rpm. Fig. 4 establishes that the adsorption efficiency increases with agitation speed. The maximum SMZ sorption (85.3%) is obtained at 300 rpm and there was no significant change in adsorption efficacy at further speeds. This effect can be attributed to the decrease in boundary layer thickness around the adsorbent particles being a result of increasing the degree of mixing(44, 45).

Effect of contact time and of initial SMZ concentration

It has reported that the mass transfer rate from the liquid to the solid phase (during adsorption processes) is influenced by contact time. The experimental results obtained for the adsorption of SMZ during various contact times are illustrated in (Fig. 5). It can be observed that the SMZ adsorbed increases with time and then attains a constant value and there is no further adsorption

after this time(46, 47). It can be inferred from these results that SMZ adsorption is performed in two stages: an initial rapid phase, which attains the saturation point within 60 min, attributed to the presence of free adsorption sites at the surface of the adsorbents. Once the SMZ are adsorbed from solution onto these sites, they block the adsorption pores (which are of smaller sizes) from subsequent adsorption. As a consequence, the adsorption speed decreases and that mark the onset of the slow second phase (step) from 60 to 90 min. Therefore, surface adsorption sites are exhausted with time. The remaining vacant sites are difficult to be occupied by the cation due to repulsive forces between adsorbate present in solid and bulk phases (48).

The effect of SMZ concentration was studied at room temperature by increasing the initial concentration of the SMZ (10-200 mg/L). It could be seen that the amount of SMZ adsorbed per unit mass (q_e) of adsorbent increased with the increase in initial concentration and contact time until equilibrium was reached at about 90 min (Fig. 6). This may be due to an increase in the number of SMZ available to be adsorbed, as well as the availability of active sites for the adsorption (49, 50). The effect of further increase in initial concentration could be studied to determine the equilibrium concentration at which the adsorbent will uptake the SMZ.

Effect of Temperature and Thermodynamic Parameters

The experiments were performed at different temperatures (283, 293, 303, 313 and 323*K*) while the other conditions has been kept constant. The percentage of adsorption increased from 19.1 to 23.2 with the increase of temperature from 283 to 323 °C at concentration of 100 mg/L and pH=7. Fig 7 indicates the results of this study. It can be found that the higher temperature facilitates the adsorption of SMZ on AF (i.e. endothermic process). This may be a result of increasing the mobility of the SMZ ion with increasing temperature. Furthermore, increasing of temperature may produce a swelling effect within the internal structure of the biosorbent which it helps the SMZ ions to further penetrate (51, 52).

Thermodynamic parameters including Gibbs free energy change (ΔG°), enthalpy change (ΔH°), and entropy change (ΔS°) is used to recognize whether the adsorption process is spontaneous or not. ΔG° were calculated from the following equation (53, 54):

$$\Delta G^\circ = -RT \ln K_d$$

Where R is the universal gas constant (8.314 J mol^{-1} K^{-1}), T is the temperature (K) and K_d is the distribution coefficient. The K_d value was calculated using following equation (55, 56):

$$K_d = \frac{q_e}{C_e}$$

Where q_e and C_e are the equilibrium concentration of SMZ on adsorbent (mg/L) and in the solution (mg/L), respectively. Relation between ΔG°, ΔH° and ΔS° can be expressed by the following equation (57):

$$\Delta G^\circ = \Delta H^\circ - T\,\Delta S^\circ$$

This equation can be written as (58):

$$\ln K_d = \frac{\Delta S^0}{R} - \frac{\Delta H^0}{RT}$$

Thermodynamic parameters (ΔH° and ΔS°), were calculated from the slope and intercept of the plot of ln K_d versus 1/T, respectively.

The ΔG°, ΔH°, and ΔS° for the adsorption of SMZ on the AF at different temperatures are given in Table 1. The negative values of ΔG° confirm the feasibility of the process and spontaneous nature of the adsorption of SMZ on the AF. On the other hand, the increasing of ΔG° with increasing temperature indicates that better adsorption is actually obtained at higher temperatures. The positive value of ΔH° confirmed the endothermic nature of adsorption, which was also supported by the increase in value of SMZ uptake of the adsorbent with the rise in temperature. Also, the values of ΔH° give an idea about the type of sorption whether the sorption is physical or chemical. The enthalpy for physical adsorption is usually no more than 8 kcal mol^{-1} and its amount for chemical adsorption is more than 8 kcal mol^{-1}; therefore, it seems that adsorption of SMZ on the AF is almost a chemical process. The positive value of $\Delta S\circ$ suggested randomness increase at the solid/solution interface during the adsorption SMZ on the AF.

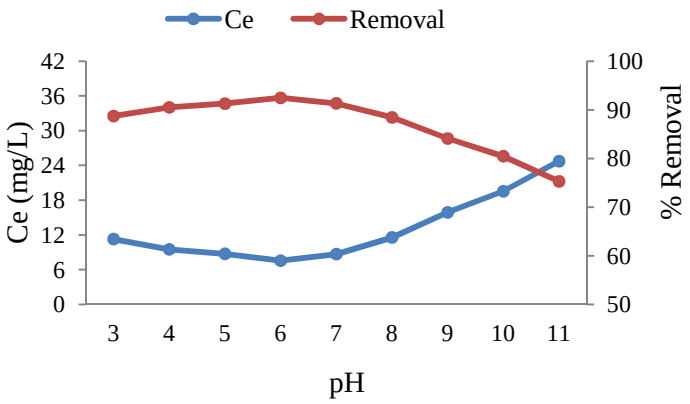

Fig. 3. Effect of pH (Dose = 2.5 g/L, SMZ concentration = 50 mg/L, Contact time 90 min and Temp= 30 ℃)

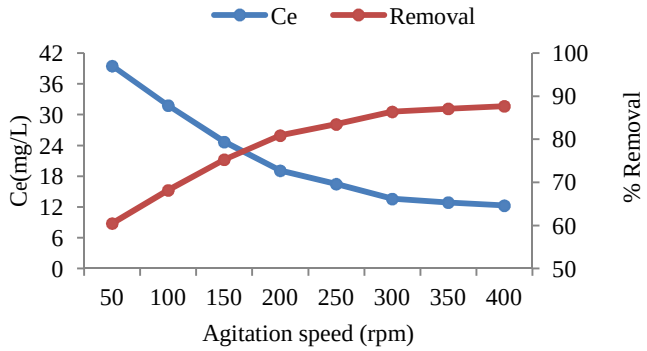

Fig. 4. Effect of agitation speed (Dose = 2.5 g/L, SMZ concentration = 100 mg/L, pH = 7, Contact time 90 min and Temp= 30 ℃)

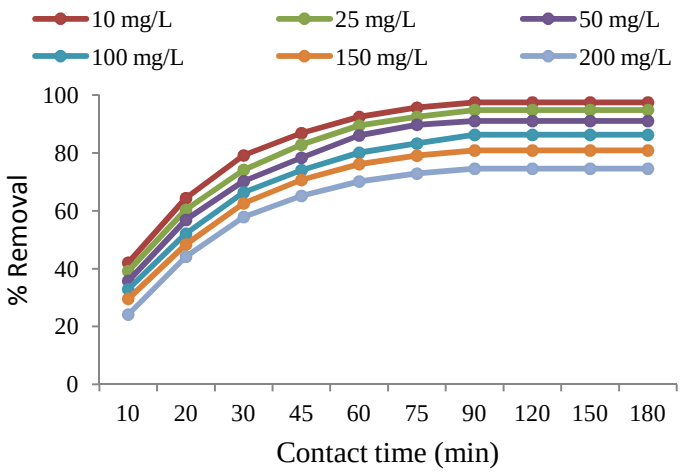

Fig. 5. Effect of Contact time and concentration on SMZ Removal (Dose = 2.5 g/L, agitation speed = 300 rpm, pH = 7 and Temp= 30 ℃)

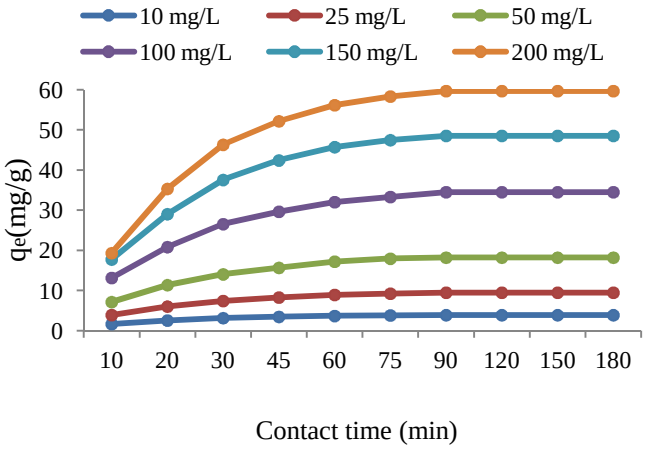

Fig. 6. The effect of contact time and SMZ concentration on adsorption capacity (Dose = 2.5 g/L, agitation speed = 300 rpm, pH = 7 and Temp= 30 ℃)

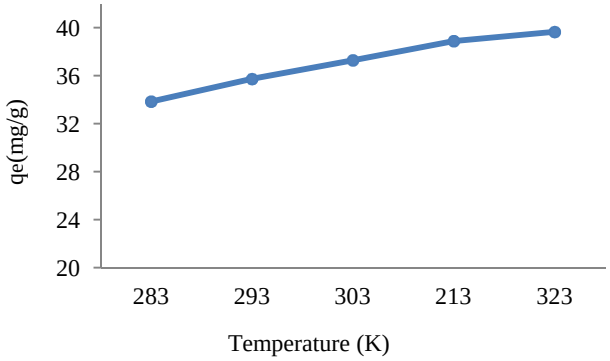

Fig. 7. Effect of temperatures on adsorption capacity (Dose = 2.5 g/L, SMZ concentration = 100 mg/L, pH = 7, Contact time 90 min and agitation speed = 300 rpm)

Table 1: Thermodynamic parameters of the SMZ adsorption on the AF at different temperatures

T (K)	(K_d)	ΔG° (kJ mol^{-1})	ΔS° (J mol^{-1} K^{-1})	ΔH° (kJ mol^{-1})
283	1.18	-0.411	45.12	9.825
293	1.49	-1.021		
303	1.76	-1.494		
313	2.07	-1.984		
323	2.46	-2.345		

Adsorption Isotherms

Adsorption isotherms describe how the adsorbates interact with adsorbents. For this purpose, three isotherm models were applied to this adsorption study. The Langmuir isotherm theory assumes monolayer coverage of adsorbate over a homogeneous adsorbent surface where all sorption sites are identical. The assumption of this theory is the uniform energies of adsorption onto the adsorbent surface. The linear form of Langmuir isotherm equation is given as follows (59, 60):

$$\frac{C_e}{q_e} = \frac{C_e}{q_{max}} + \frac{1}{q_{max}\, K_L}$$

Where q_e (mg/g) is the amount of SMZ adsorbed per unit mass of adsorbent at equilibrium, C_e (mg/L) is the final concentration at equilibrium, q_{max} (mg/g) is the maximum adsorption at monolayer coverage and K_L (L/mg) is the constant related to the extent of adsorption. The parameter calculated from the Langmuir model isotherm is given in Table 2. The high correlation coefficient obtained from Langmuir model confirms that the this isotherm might be suitable for the interpretation of the adsorption data. The essential features of Langmuir can be expressed by a dimensionless constant which is called separation factor or equilibrium parameter (R_L) and is calculated using the following equation (61):

$$R_L = \frac{1}{1+C_0 K_L}$$

Where C_0 (mg/L) is the initial concentration of the SMZ. The values of R_L indicate the shapes of isotherms which it can be either unfavorable ($R_L>1$), linear ($R_L=1$), favorable ($0<R_L<1$). In the present investigation the equilibrium parameter (Table 2) was found to be in the range $0<R_L<1$ (between 0.081-0.185) indicating that the adsorption process was favorable and the Langmuir isotherm was applicable ($R^2>0.996$ at all temperatures).

The Freundlich isotherm assumes that the adsorption process takes place on heterogeneous surfaces and the adsorption capacity is related to the concentration of the adsorbent. The Freundlich model is based on the following expression (62, 63):

$$\text{Ln } q_e = \ln K_F + \frac{1}{n} \ln C_e$$

The constant K_F is an approximate indicator of adsorption capacity while 1/n is a function which is related to the strength of adsorption in the adsorption process. If the value of n is equal with 1, the partition between the two phases are independent of the concentration. When the value of 1/n is below 1, the adsorption is occurred normally. On the other hand, the cooperative adsorption

can be observed. In addition, the value of n between one and ten indicates a favorable sorption process. As it can be seen in table 2, the values of n is higher than 1.8 at all temperatures which it indicates the favorable sorption of SMZ and the R^2 value is above of 0.85.

Temkin Isotherm: This isotherm contains a factor that explicitly taking into the account of adsorbent–adsorbate interactions. This model assumes that heat of adsorption (function of temperature) of all molecules in the layer would reduce linearly with coverage and it is not dependent to the concentration. The model is shown by the following equation (64):

$$q_e = \frac{RT}{B} \ln A + \frac{RT}{B} \ln C_e$$

Where A is Temkin isotherm equilibrium binding constant (L/g); B is Temkin isotherm constant; R is universal gas constant (8.314J/mol/K); T is temperature (K). The comparing of the correlation coefficients (R^2) at all temperatures obtained from the three isotherms (Table 2) reveals that Langmuir model can be applied successfully to explain the equilibrium data of adsorption of SMZ on AF biomass. Increase in temperature causes an increase in the mobility of SMZ and the kinetic energies of SMZ increased, leading in turn to an increase in the adsorption of SMZ onto AF.

Table 2: Isotherm parameters for SMZ adsorption onto AF biomass

Tem ($°K$)	283	293	303	313	323
Langmuir					
q_{max}(mg/g)	30.81	32.18	33.95	35.44	37.86
K_L (L/mg)	0.044	0.068	0.091	0.104	0.112
R_L	0.185	0.128	0.099	0.088	0.081
R^2	0.997	0.996	0.997	0.999	0.998
Freundlich					
K_F (mg/g)	4.451	5.844	5.976	6.435	7.382
n	1.85	2.27	2.68	2.94	3.29
R^2	0.855	0.876	0.884	0.895	0.871
Temkin					
A (L/g)	0.125	0.176	0.241	0.285	0.314
B	28.45	29.11	30.72	31.66	32.39
R^2	0.795	0.774	0.832	0.814	0.859

Adsorption Kinetics

Adsorption kinetics show large dependence on the physical and chemical characteristics of the adsorbent material and presence of adsorbate in bulk. In the present work, pseudo first-order, pseudo second-order and intraparticle diffusion kinetic models were used in order to examine the controlling mechanism of sorption processes such as mass transfer and chemical reaction.

Pseudo-first order kinetic model

The linear form of first-order kinetic equation is (65, 66):

$$\text{Log } (q_e - q_t) = \log q_e - \frac{K_1}{2.303} t$$

Where q_e and q_t are the amounts of SMZ adsorbed at equilibrium and at time t (min) respectively; k_1 is the first-order rate constant (min^{-1}). A straight line of $ln(q_e-q_t)$ versus t suggests the applicability of this kinetic model, and q_e and k_1 can be determined from the intercept and slope of the plot, respectively. The results of the Pseudo-first order kinetic parameters are given in Fig 8a and Table 3. The result showed that the adsorption of SMZ onto AF did not follow the first order kinetics. At the given temperature, the first-order rate constant (k_1) increased with the increasing of initial SMZ concentration. At higher initial SMZ concentration, the number of available binding sites at the AF surface per adsorbate molecule increased. The adsorption data fitted poorly with pseudo-first order kinetic model for AF biomass and the calculated q_e values did not agree with the experimental q_e values at all concentrations.

Pseudo-second order kinetic model

Pseudo second-order model rate equation is represented as (67):

$$\frac{t}{q_t} = \frac{1}{k_2 q_e^2} + \frac{t}{q_e}$$

Where k_2 (g mg^{-1} min^{-1}) is the rate constant of the second-order equation. A straight line of t/q_t versus t suggests the applicability of this kinetic model, and q_e and k_2 can be determined from the intercept and slope of the plot, respectively (Fig 8b). Table 3 shows the obatined data from pseudo-second-order model. It is observed from Table 3 that there was a good agreement between experimental q_e and calculated q_e values with high correlation coefficient values for adsorbent. Hence the pseudo second-order model better represented the adsorption kinetics between the AF biomass and SMZ. The adsorption process is depended on the concentration of adsorbent and adsorbate. The rate of adsorption depended on the concentration of AF and SMZ molecules in the bulk.

Intraparticle diffusion

The adsorption kinetic data were further processed to explore the possibility of intra-particle diffusion using the Weber–Morris equation. The model is expressed by the following equation (68):

$$q_t = k_{dif}\, t^{0.5} + C$$

Where K_{dif} is the intra-particle diffusion rate constant (mg/g min½) and C is the boundary layer thickness.

The Weber-Morris intraparticle diffusion model was commonly used to determine the sorption data, which was used to study the diffusion mechanism during the adsorption process. A linear plot of q_t versus $t^{1/2}$ at different initial concentrations is shown in Fig. 8c and the parameters are given in Table 3. As can be seen from Fig. 8c, the diffusion kinetic plots exhibited the three-stage linearity. It has a good linear correlation between q_t and $t^{1/2}$ in this stage, indicating that the adsorption process was not only controlled by intra-particle diffusion, but two or more steps were controlling the adsorption process. The first portion of curve has sufficient available adsorption sites on the adsorbents surface with high adsorption rate; this portion was ascribed to the diffusion of SMZ molecule in micropores biomass. Afterwards, the second linear portion

belongs to intraparticle diffusion. The SMZ molecules come across much larger hindrance because of transfer in deeper inner pores. Then the third section represented final equilibrium stage where the intra-particle diffusion begins to slow down the arrival of absorption saturation, and the diffusion of SMZ molecules into micropores biomass. Furthermore, the plot of line did not pass through the origin. This results suggested that the boundary layer control was involved in this adsorption stage. The value of C increased with the increasing of the initial concentration, indicating that the film diffusion plays more important role at high initial concentration(40, 41). These results also implied that this mechanism does not individually limit the overall adsorption process, which may be a complicated combination of involving both surface adsorption and intra-particle diffusion.

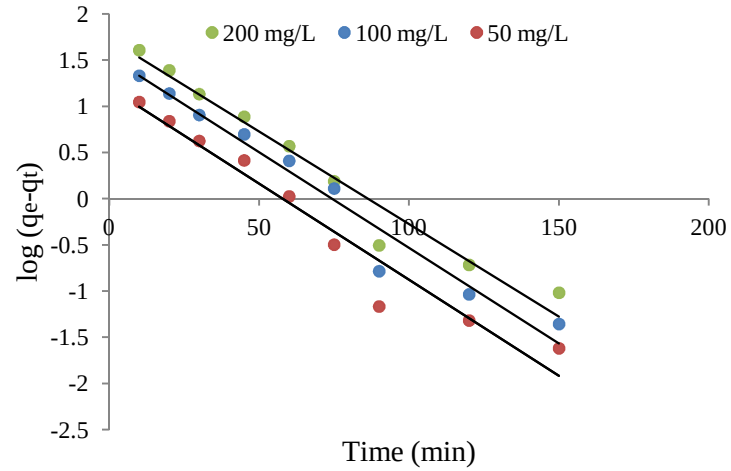

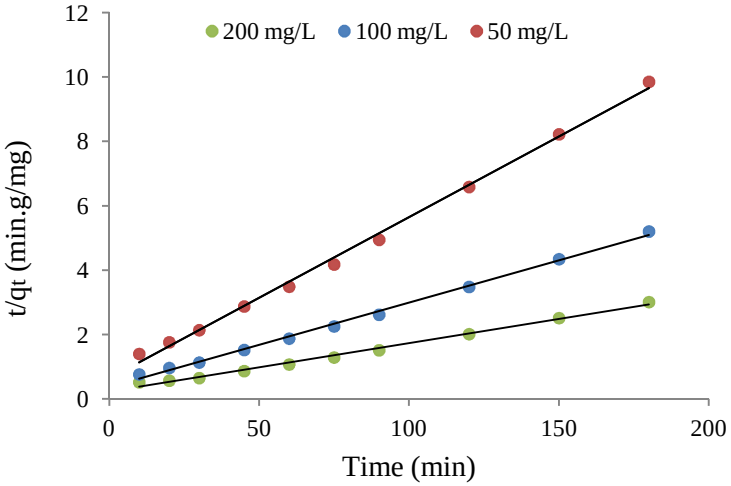

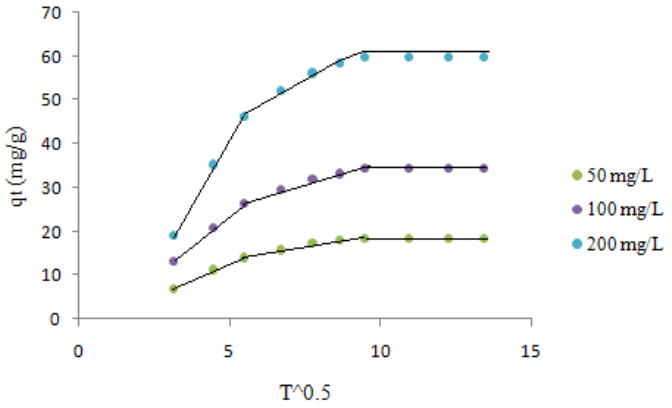

Fig. 8. Adsorption kinetics of SMZ on AF a: pseudo-first-order b: pseudo-second-order C: intra-particle diffusion

Table 3: Kinetic parameters for the adsorption of SMZ onto AF biomass at various concentration

C_o(mg/L)	$q_{e\ exp}$ (mg/g)	Pseudo-first order			Pseudo-second order			Intraparticle diffusion		
		K_1	q_e	R^2	K_2	q_e	R^2	k_{dif}	C	R^2
50	18.22	0.0564	13.58	0.806	0.0723	17.85	0.998	0.193	1.876	0.783
100	34.52	0.0725	29.47	0.864	0.0464	33.69	0.999	0.245	2.244	0.775
200	59.66	0.0867	52.64	0.882	0.0221	58.76	0.996	0.326	2.957	0.794

Conclusion: In the present study, batch adsorption experiments have been carried out for the adsorption of SMZ from aqueous solutions using AF biomass. The effects of various parameters such as contact times, temperature, pH, initial SMZ concentrations and agitation speed were investigated. The isotherm studies revealed that the equilibrium data obtained from for the adsorption of SMZ on AF biomass was better described by Langmuir isotherm model compared with Freundlich and Temkin model. In addition, the thermodynamic studies indicated that SMZ adsorption process onto the AF is endothermic and spontaneous. Furthermore, Kinetics of adsorption process was investigated using pseudo first order kinetic, pseudo second order and intraparticle diffusion kinetic models. The results showed that the adsorption process followed pseudo second order kinetic model. Finally, this study revealed that AF biomass can be effectively used for the adsorption of Sulfamethoxazole antibiotics from aqueous solution.

References:

1. Su YF, Wang GB, Kuo DTF, Chang ML. Photoelectrocatalytic degradation of the antibiotic sulfamethoxazole using TiO_2/Tiphotoanode. Applied Catalysis B: Environmental. 2016; 186;184-92.
2. Balarak D, Mostafapour FK, Joghataei A. Experimental and Kinetic Studies on Penicillin G Adsorption by Lemna minor. British Journal of Pharmaceutical Research.2016; 9(5): 1-10.
3. Rostamian R, Behnejad H. A comparative adsorption study of sulfamethoxazole onto graphene and graphene oxide nanosheets through equilibrium, kinetic and thermodynamic modeling. Process Safety and Environmental Protection.2016;102;20-29.
4. Hu L, Flanders PM, Miller PL, Strathmann TJ. Oxidation of sulfamethoxazole and related antimicrobial agents by TiO_2 photocatalysis Water Research 2007;41(12); 2612-26.
5. Yu F, Li Y, Han S, Jie Ma J. Adsorptive removal of antibiotics from aqueous solution using carbon Materials. Chemosphere. 2016;153;365–85.
6. Garoma T, Umamaheshwar SH, Mumper A. Removal of sulfadiazine, sulfamethizole, sulfamethoxazole, and sulfathiazole from aqueous solution by ozonation. Chemosphere. 2010;79;814–20.

7. Rostamian R, Behnejad H. A comparative adsorption study of sulfamethoxazole onto graphene and graphene oxide nanosheets through equilibrium, kinetic and thermodynamic modeling. Process Safety and Environmental Protection.2016;102;20-29.
8. Johnson MB, Mehrvar M. Aqueous metronidazole degradation by UV/H_2O_2 process in single-and multi-lamp tubular photoreactors: kinetics and reactor design, Ind. Eng. Chem. Res.2008; 47; 6525–37.
9. Choi KJ, Kim SG, Kim SH. Removal of antibiotics by coagulation and granular activated carbon filtration. J. Hazard. Mater.2008; 151;38–43.
10. Hao Chena H, Bin Gaoa B, Lib H. Removal of sulfamethoxazole and ciprofloxacin from aqueous solutions by graphene oxide. Journal of Hazardous Materials.2015;283;201-07.
11. Zhang W, He G, Gao P, Chen G: Development and characterization of composite nanofiltration membranes and their application in concentration of antibiotics. Sep Purif Technol 2003, 30:27–35.
12. Balarak D, Mahdavi Y and Mostafapour FK. Application of Alumina-coated Carbon Nanotubes in Removal of Tetracycline from Aqueous Solution. British Journal of Pharmaceutical Research.2016; 12(1): 1-11.
13. Balarak D, Azarpira H, Mostafapour FK. Study of the Adsorption Mechanisms of Cephalexin on to Azolla Filiculoides. Der Pharma Chemica, 2016, 8(10):114-121
14. Gulkowsk A, Leung HW, So MK, Taniyasu S, Yamashita N. Removal of antibiotics from wastewater by sewage treatment facilities in Hong Kong and Shenzhen, China. Water research. 2008;42:395-403.
15. Zhang W, He G, Gao P, Chen G: Development and characterization of composite nanofiltration membranes and their application in concentration of antibiotics. Sep Purif Technol 2003, 30:27–35
16. Zhu XD, Wang YJ, Sun RJ, Zhou DM. Photocatalytic degradation of tetracycline in aqueous solution by nanosized TiO_2. Chemosphere. 2013; 92; 925–32.
17. Balarak D, Azarpira H,. Rice husk as a Biosorbent for Antibiotic Metronidazole Removal: Isotherm Studies and Model validation. International Journal of ChemTech Research. 2016; 9(7); 566-573.
18. Ali I. New generation adsorbents for water treatment. Chem. Revs. 2012;112:5073-509.
19. Aksu Z, Tunc O. Application of biosorption for Penicillin G removal: Comparison with activated carbon. Process Biochemistry. 2005;40(2):831-47.
20. Balarak D, Mahdavi Y, Maleki A, Daraei H and Sadeghi S. Studies on the Removal of Amoxicillin by Single Walled Carbon Nanotubes. British Journal of Pharmaceutical Research. 2016;10(4): 1-9.
21. Putra EK, Pranowoa R, Sunarsob J, Indraswatia N, Ismadjia S. Performance of activated carbon and bentonite for adsorption of amoxicillin from wastewater: mechanisms, isotherms and kinetics. Water Res. 2009; 43, 2419-30.
23. Zhang L, Song X, Liu X, Yang L, Pan F, Lv J. Studies on the removal of tetracycline by multi-walled carbon nanotubes, Chem. Eng. J. 2011; 178; 26–33.
24. Ahmed MJ, Theydan SK. Adsorption of cephalexin onto activated carbons from Albizia lebbeck seed pods by microwave-induced KOH and K_2CO_3 activations. Chemical Engineering Journal.2012;211-212; 200-7.
25. Gao J and Pedersen JA. Adsorption of Sulfonamide Antimicrobial Agents to Clay Minerals. Environ. Sci. Technol. 2005, 39(24). 9509-16.
26. Dutta M, Dutta NN, Bhattachary KG. Aqueous phase adsorption of certain beta-lactam antibiotics onto polymeric resins and activated carbon. Separation and Purification Technology.1999;16(3);213-24.
27. Peterson JW. Petrasky LJ, Seymourc MD, Burkharta RS, Schuilinga AB. Adsorption and breakdown of penicillin antibiotic in the presence of titanium oxide nanoparticles in water. Chemosphere. 2012;87(8); 911-7.
28. Chen WR, Huang CH. Adsorption and transformation of tetracycline antibiotics with aluminum oxide. Chemosphere. 2010; 79, 779-85.

29. Xu L, Pan J, Dai J, Li X, Hang H, Cao Z, Yan Y. Preparation of thermal-responsive magnetic molecularly imprinted polymers for selective removal of antibiotics from aqueous solution. Journal of Hazardous Materials. 2012; 233-234;48-56.
30. Rivera-Jiménez SM, Hernández-MaldonadoAJ. Nickel(II) grafted MCM-41: A novel sorbent for the removal of Naproxen from water. Microporous and Mesoporous Materials. 2008;116(1-3); 246‑52.
31. Adrianoa WS, Veredasb V, Santanab CC, Gonçalves LRB. Adsorption of amoxicillin on chitosan beads: Kinetics, equilibrium and validation of finite bath models. Biochemical Engineering Journal. 2005; 27(2) ;132-37.
32. Erşan M, Bağd E. Investigation of kinetic and thermodynamic characteristics of removal of tetracycline with sponge like, tannin based cryogels. Colloids and Surfaces B: Biointerfaces. 2013;104;75-82.
33. Balarak D, Mostafapour FK. Canola Residual as a Biosorbent for Antibiotic Metronidazole Removal. The Pharmaceutical and Chemical Journal, 2016, 3(2):12-17.
34. Zazouli MA, Mahvi AH, Dobaradaran S, Barafrashtehpour M, Mahdavi Y, Balarak D. Adsorption of fluoride from aqueous solution by modified Azolla Filiculoides. Fluoride. 2014;47(4):349-58.
35. Zazouli MA, Mahdavi Y, Bazrafshan E, Balarak D. Phytodegradation potential of bisphenolA from aqueous solution by Azolla Filiculoides. Journal of Environmental Health Science & Engineering 2014;12(66):1-5.
36. Balarak D, Joghataei A, Azadi NA, Sadeghi S. Biosorption of Acid Blue 225 from Aqueous Solution by Azolla filiculoides: Kinetic and Equilibrium Studies. American Chemical Science Journal. 2016; 12(2):1-10.
37. Padmesh TVN, Vijayaraghavan K, Sekaran G, Velan M. Batch and column studies on biosorption of acid dyes on fresh water macro alga Azolla filiculoides. J Hazardous Mat. 2005; 4(125):121-9.
38. Pandey VC. Phytoremediation of heavy metals from fly ash pond by Azolla caroliniana. Ecotoxicology and Environmental Safety.2012:82:8-12.
39. Diyanati RA, Yousefi Z, Cherati JY, Balarak D. Adsorption of phenol by modified azolla from Aqueous Solution. Journal of Mazandaran University of Medical Science. 2013; 22(2);13-21.
40. Diyanati RA, Yousefi Z, Cherati JY, Balarak D. The ability of Azolla and lemna minor biomass for adsorption of phenol from aqueous solutions. J Mazandaran Uni Med Sci. 2013; 23(106).17-23.
41. Zazouli MA, Balarak D, Mahdavi Y. Effect of Azolla filiculoides on removal of reactive red 198 in aqueous solution. J Adv Environ Health Res. 2013; 1(1):1-7.
42. Balarak D, Bazrafshan E, Kord Mostafapour F. Equilibrium, Kinetic Studies on the Adsorption of Acid Green 3(AG3) Dye Onto Azolla filiculoides as Adosorbent. American Chemical Science Journal.2016;11(1);1-10.
43. Zazouli MA, Yazdani J, Balarak D, Ebrahimi M, Mahdavi Y. Removal Acid Blue 113 from Aqueous Solution by Canola. Journal of Mazandaran University Medical Science. 2013;23(2):73-81.
2002;84;291-93.
45. Crini G, Peindy HN, Gimbert F, Robert C. Removal of C.I. Basic Green 4 (Malachite Green) from aqueous solutions by adsorption using cyclodextrin-based adsorbent: Kinetic and equilibrium studies. Separation and Purification Technology. 2007;53;97-110.
46. Balarak D, Mahdavi Y. Survey of Efficiency Agricultural Waste as Adsorbent for Removal of P-Cresol from Aqueous Solution. International Research Journal of Pure & Applied Chemistry. 2016; 10(2): 1-11.
47. Ghauch A, Tuqan A, Assi HA: Elimination of amoxicillin and ampicillin by micro scale and nano scale iron particles. Environ Pollut 2009,157:1626–35.
48. Peng X, Hu F, Dai H, Xiong Q. Study of the adsorption mechanism of ciprofloxacin antibiotics onto graphitic ordered mesoporous carbons. Journal of the Taiwan Institute of Chemical Engineers.2016; 8; 1–10.
49. Balarak D, Mostafapour FK, Joghataei A. Adsorption of Acid Blue 225 dye by Multi Walled Carbon Nanotubes: Determination of equilibrium and kinetics parameters. Der Pharma Chemica, 2016, 8(8):138-145.

50. Upadhyayula VKK, Deng S , Mitchell MC, Smith GF. Application of carbon nanotube technology for removal of contaminants in drinking water: A review. Science of the Total Environment. 2009; 408;1-13.
51. Balarak D, Joghataei A. Biosorption of Phenol using dried Rice husk biomass: Kinetic and equilibrium studies. Der Pharma Chemica, 2016, 8(6):96-103.
52. Gao Y, Li Y, Zhang L, Huang H, Hu J, Shah SM, Su X. Adsorption and removal of tetracycline antibiotics from aqueous solution by graphene oxide, J. Colloid. Interface Sci. 2012; 368; 540-46.
53. Balarak D, Jaafari J, Hassani G, Mahdavi Y, Tyagi I, Agarwal S, Gupta VK. The use of low-cost adsorbent (Canola residues) for the adsorption of methylene blue from aqueous solution: Isotherm, kinetic and thermodynamic studies. Colloids and Interface Science Communications. Colloids and Interface Science Communications. 2015;7:16–19.
54. Malakootian M, Balarak D, Mahdavi Y, Sadeghi SH, Amirmahani N. Removal of antibiotics from wastewater by azolla filiculoides: kinetic and equilibrium studies. International Journal of Analytical, Pharmaceutical and Biomedical Sciences. 2015;4(7);105-113.
55. Balarak D, Mahdavi Y, Bazrafshan E, Mahvi AH, Esfandyari Y. Adsorption of fluoride from aqueous solutions by carbon nanotubes: Determination of equilibrium, kinetic and thermodynamic parameters. Flouride. 2016;49(1):35-42.
56. Mohammadi AS, Sardar M. The Removal of Penicillin G from Aqueous Solutions using Chestnut Shell Modified with $H2_SO_4$: Isotherm and Kinetic Study. Journal of Health & Environmental. 2012;6(1):497-508.
58 Balarak D, Mahdavi Y, Bazrafshan E , Mahvi AH. Kinetic, isotherms and thermodynamic modeling for adsorption of acid blue 92 from aqueous solution by modified azolla filicoloides. Fresenius Environmental Bulletin.2016;25(5); 1321-30.
59. Ali I. The quest for active carbon adsorbent substitutes: Inexpensive adsorbents for toxic metal ions removal from wastewater. Sepn. & Purfn. Rev. 2010;39(3-4):91-171.
60. Zazouli MA, Mahvi AH, Mahdavi Y, Balarak D. Isothermic and kinetic modeling of fluoride removal from water by means of the natural biosorbents sorghum and canola. Fluoride. 2015;48(1):15-22.
61. Balarak D. Kinetics, Isotherm and Thermodynamics Studies on Bisphenol A Adsorption using Barley husk. International Journal of ChemTech Research. 2016;9(5);681-90.
62. Tor A, Cengeloglu Y. Removal of congo red from aqueous solution by adsorption onto acid activated red mud. Journal of Hazardous Materials. 2006;138(2):409-15.
63. Low KS, Lee CK, Tan BF. Quaternized wood as sorbent for reactive dyes. Biochem Biotechnol. 2000;87:233-45.
64. Balarak D, Azarpira H, Mostafapour FK. Thermodynamics of removal of cadmium by adsorption on Barley husk biomass. Der Pharma Chemica, 2016,8(10):243-47.
65. Khaled A, Nem AE, El-Sikaily A, Abdelwahab O. Removal of Direct N Blue- 106 from artificial textile dye effluent using activated carbon from orange peel: adsorption isotherm and kinetic studies, J. Hazard. Mater. 2009: 165 ;100-10.
66. Haq I. Bhatti HN. Asgher M. Removal of solar red BA textile dye from aqueous solution by low cost barley husk: Equilibrium, kinetic and thermodynamic study.Canadian Journal of Chemical Engineering. 2011; 89(3);593–600.
67. Ali I, Asim M, Khan TA. Low cost adsorbents for the removal of organic pollutants from wastewater. J. Environ. Manag.2012; 113: 170-183.
68. Robinson T. Chandran B. Nigam P. Removal of dyes from an artificial textile dye effluent by two agricultural waste residues, corncob and barley husk. Environment International. 2002; 28(1-2);29–33.